2011

High-resolution surveys of internal tidal waves in Monterey Bay, California, using an autonomous underwater vehicle

Cazenave, François

LIMNOLOGY
and
OCEANOGRAPHY: METHODS

Limnol. Oceanogr.: Methods 9, 2011, 571–581

High-resolution surveys of internal tidal waves in Monterey Bay, California, using an autonomous underwater vehicle

François Cazenave[1], Yanwu Zhang[1], Erika McPhee-Shaw[2], James G. Bellingham[1], and Timothy P. Stanton[3]*
[1]Monterey Bay Aquarium Research Institute, 7700 Sandholdt Road, Moss Landing, CA 95039, USA
[2]Moss Landing Marine Laboratories, California State University, 8272 Moss Landing Road, Moss Landing, CA 95039, USA
[3]Naval Postgraduate School, Department of Oceanography, Monterey, CA 93943, USA

Abstract

Temperature measured at the Monterey Inner Shelf Observatory (MISO) in southern Monterey Bay reveals frequent solitons and semidiurnal internal tidal bores (ITBs). A field study was undertaken to determine whether these features originate offshore and propagate shoreward over the continental shelf, and to characterize their evolution as they propagate. We developed a new survey method of using an autonomous underwater vehicle (AUV) to tightly track the thermocline along a 4.5 km transect, repeated 18 times over 18 hours, thereby measuring the internal-wave induced isotherm displacement at very high resolution. AUV measurements were compared with measurements at MISO, which is closer to shore. Internal waves of various scales were captured. An ITB of amplitude greater than 20 m propagating shoreward from the outer bay was the dominant feature. Rapid changes in stratification, possibly due to horizontal advection, were also observed. Technical challenges, advantages, and future improvements of this new AUV survey method are discussed. This study demonstrates that AUVs are efficient tools for surveying internal tidal waves.

Nonlinear internal waves are commonly observed on continental shelves throughout the world (Holloway et al. 1999; Colosi et al. 2001; MacKinnon and Gregg 2003; Stanton and Ostrovsky 1998; Small and Martin 2002; Scotti et al. 2008; Shroyer et al. 2009). They often exhibit features such as solitary waveforms and high amplitude displacement over short time scales (<1 h), and they often occur in groups whose repetition period (the interval between successive groups) is tidal. Nonlinear internal waves can have important effects on coastal biological processes by promoting vertical mixing within and near the euphotic zone. Alternating convergent and divergent surface currents associated with propagation of internal bores can generate slicks at the sea surface, and at depth can affect the distribution and aggregation of dinoflagellates and other plankton (Cheriton et al. 2009). Vertical internal-wave transport of phytoplankton in and out of the euphotic zone can have important consequences for phytoplankton growth and cell division (Lennert-Cody and Franks 2002). Shoaling internal waves have been shown to be an important mechanism for delivering nutrients to inner shelf kelp ecosystems (McPhee-Shaw et al. 2007) and to coral reefs (Leichter et al. 2003).

Nonlinear internal waves have been observed extensively on the continental shelf of Monterey Bay, California. Carter et al. (2005) found evidence that the mid and outer Monterey Bay shelf was populated by internal waves generated by conversion of barotropic tidal energy to baroclinic tidal energy at the shelf break. Many features had solitary-wave characteristics, and solitary waves of both elevation and depression were observed (Carter et al. 2005). Persistent and intense motions associated with nonlinear internal waves have also been observed at the Monterey Inner Shelf Observatory (MISO) located at 12-m depth in the southern portion of the Bay near Monterey (Tjoa 2003). These waves were characterized by abrupt drops in temperature of up to 4°C followed by rapid oscillations. Features of these waves include characteristics of both "solitary" waves (thermocline depth varying over 4 m in less than 10 min, for example), and of lower-frequency, longer wavelength semidiurnal internal tides. In this article, we will

*Corresponding author: E-mail: francois@mbari.org

Acknowledgments

This work was supported by the David and Lucile Packard Foundation. The authors are thankful to Thomas Hoover for his work in planning and conducting the Dorado AUV surveys, to Robert McEwen for helping incorporating the isotherm-following algorithm into the AUV code, to William Shaw for insightful discussions on internal waves, and to Kenneth Coale for his help and advice. Hard work of the MBARI AUV operations personnel Hans Thomas, Duane Thompson, Douglas Conlin, and the R/V *Zephyr* crew is much appreciated. The authors also appreciate the help from Jim Stockel and Kim Fulton-Bennett.

DOI 10.4319/lom.2011.9.571

use the term "internal tidal bore (ITB)" to refer to a semidiurnal-period, solitary waveform disturbance of thermocline isopycnals, whereas the term "soliton" refers to a short period (15 min to 1 h), highly nonlinear, steep disturbance of the isopycnal (e.g., Stanton and Ostrovsky 1998).

Nonlinear internal waves are highly variable in space and time. Coarse spatial resolution of moorings and shipboard measurements limits our ability to characterize the fine scales. Autonomous underwater vehicles (AUVs), as cost-effective mobile platforms, can provide high-resolution measurements in both time and space. We developed a new method for an AUV to closely track individual isotherms and make very high-resolution measurements of internal tidal waves as they propagate over the continental shelf. Our objective was to assess the application of AUVs for studying nonlinear internal waves, because a long-term goal is to use AUVs to first identify an internal wave feature, and then to track its propagation while simultaneously measuring the progress of biological processes within a solitary bore, or within the larger wave packet as it moves across the shelf.

Using the new method, a Dorado AUV was programmed to tightly track within two isotherms of the thermocline, continuously flying offshore and onshore along a 4.5-km transect that was repeated about once per hour over about 18 h. This allowed the AUV to closely follow any internal-wave induced isotherm displacements during the 18 h survey. Two AUV surveys were carried out to sample internal tidal waves propagating over the shelf and to help determine the origin of those observed at the inner-shelf MISO site. In an AUV mission on 14-15 May 2007 on the mid-shelf, the AUV recorded a strong ITB on the mid shelf. The same ITB was also recorded inshore at the MISO station, and the two data sets together suggest shoreward propagation of an ITB. This study demonstrated that AUVs can be efficient tools for sampling internal waves.

Materials and procedures

A new method of tracking the thermocline with an AUV

Internal tidal waves are highly variable in time and space. Consequently, studying them requires high-resolution measurements in both time and space. Spatial resolution of measurements by moorings or ships is limited by the number of stations because equipment and logistics costs are high. AUVs are cost-effective mobile platforms that can provide high-resolution measurements in both time and space. The Dorado AUV (Bellingham et al. 2000; Thompson 2007) developed at the Monterey Bay Aquarium Research Institute (MBARI) is a propeller-driven vehicle with a length of 4.2 m and a diameter of 0.53 m at the midsection. At a typical speed of 1.5 m/s, the vehicle can travel about 100 km on about 20 h of battery life. The AUV's sensor suite includes temperature, conductivity, pressure, chemical, optical, and acoustic sensors. The data are recorded by the vehicle's onboard computer and can be downloaded by radio once the AUV is on the surface or via an Ethernet connection after the AUV is recovered.

A common AUV survey mode is to fly on a saw-tooth trajectory in the vertical plane within a preset depth envelope. Bird et al. (1997) observed internal waves in a lake by running an AUV on a saw-tooth trajectory between 10-m to 20-m depths. There is a dilemma in setting a fixed depth envelope for the AUV: if it is set too narrow, the vehicle may easily miss the thermocline; if it is set too wide, the spacing between the vehicle's successive crossings of the thermocline will be large so the spatial resolution will be poor. In this article, we present a new method for an AUV to tightly track an isotherm (the thermocline), thereby making very high-resolution measurements of the internal tidal waves as they propagate over the continental shelf. We developed a new AUV behavior algorithm (a computer function) to command the vehicle to fly on a saw-tooth trajectory within a narrow temperature envelope instead of within a fixed-depth envelope. Author Bellingham devised this method and used it in Odyssey AUV surveys in the Massachusetts and Cape Cod Bays in 1998, but the method was not published. We are unaware of any similar AUV survey mode reported in the literature.

The new AUV flying behavior is depicted as follows: Before each full survey, the AUV was first run along a short saw-tooth transect over a depth range that sufficiently covered the water column. On completion of the short mission, when the vehicle was at the surface, data were downloaded by a radio link, and we quickly reviewed the temperature profile to identify the thermocline and accordingly determine the lower and upper temperature bounds for the ensuing full survey. Suppose the temperature decreases with depth. When the diving vehicle hits the lower temperature bound, it switches from diving to climbing. On its climb, upon hitting the upper temperature bound, the AUV switches from climbing back to diving. If we set the lower and upper temperature bounds close to each other, the AUV will effectively track an isotherm. The closer the two bounds, the more frequent the vertical turns of the vehicle. The ultimate closeness of the two bounds is limited by the vehicle's control dynamics in the vertical plane. For example, in the AUV survey on 14-15 May 2007, the lower and upper temperature bounds were set to 10.1°C and 10.3°C, respectively. Thus in the internal wave field, the AUV closely tracked the rises and drops of the thermocline.

In 2007, we carried out AUV surveys in Monterey Bay, California, using this method (Fig. 1). Surveys were done during spring tides, which may be more favorable for internal tidal wave generation in this region (Petruncio et al. 1998; Stanton and Ostrovsky 1998). To increase the chance of capturing internal waves, surveys were set up for a full, overnight, 18-h duration. The low-frequency internal waves previously recorded at MISO had semidiurnal periods around 12 h, so an 18-h survey was supposed likely to capture at least one internal tide event. Throughout each survey, the AUV ran back and forth on a 4.5-km cross-shelf transect. It took the vehicle about 1 h to "sweep" the transect once, so during each survey the vehicle was able to sweep the transect approximately 18

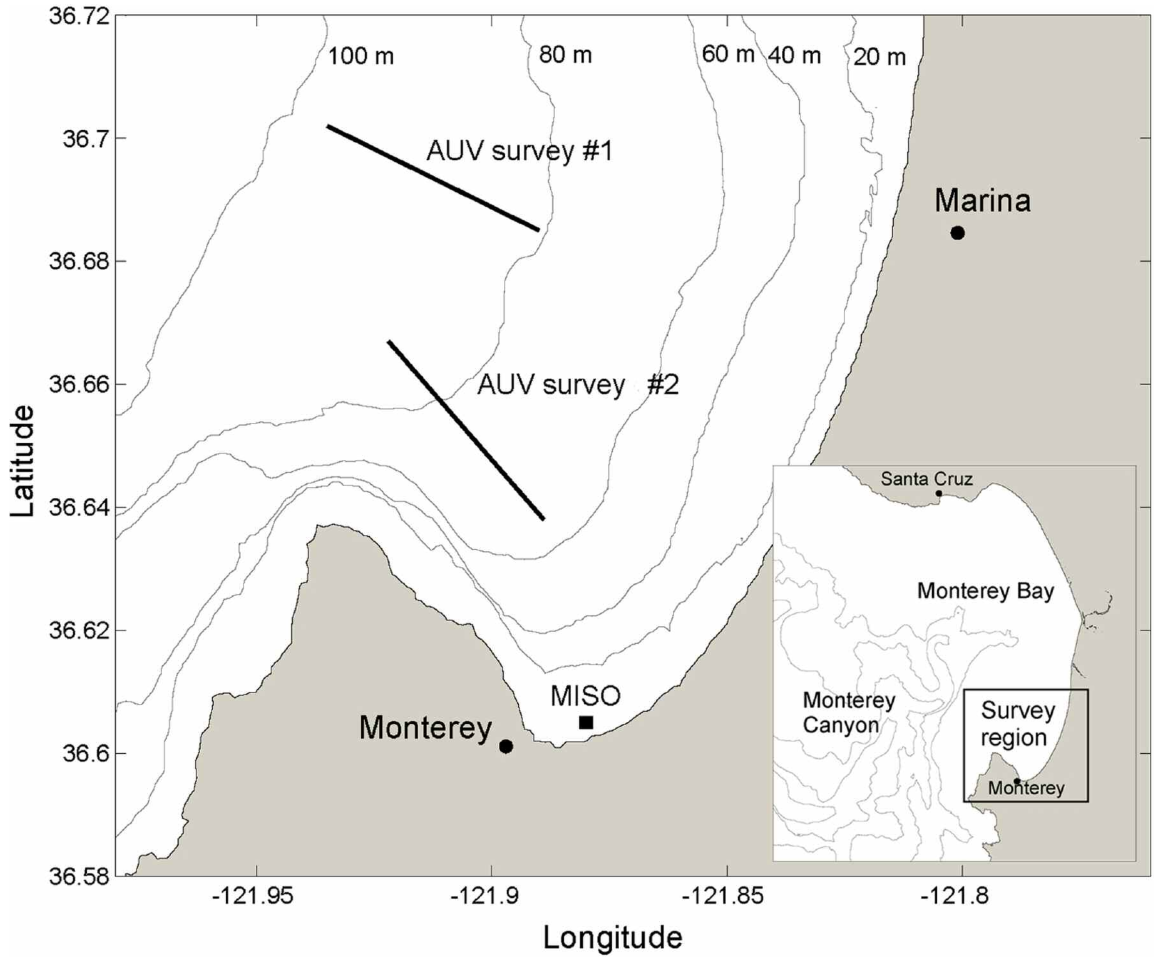

Fig. 1. Map of surveys.

times. Each 1-h sweep can be viewed as a snapshot of the thermocline on the transect.

Monterey Inner Shelf Observatory data

The Monterey Inner Shelf Observatory (MISO, http://www.oc.nps.edu/~stanton/miso/) is an underwater cabled observatory located in southern Monterey Bay, 600 m offshore. The water depth at the station is 12 m. It is connected via a cable to a land station that provides power and Ethernet connectivity, allowing immediate access to the data. It was designed and deployed in 2000 by author Stanton and the Ocean Turbulence Research group at the Naval Postgraduate School in Monterey. A chain of 16 thermistors measures water temperature at 1-m intervals between 0.5 and 8.6 m above the seafloor. Tide height was measured by a high-precision digital pressure sensor (Paroscientific).

Semi-diurnal ITBs appear at MISO on a daily basis from early spring to late fall, with varying intensity. They appear as rapid drops of temperature (up to 4°C) usually followed by rapid oscillations. These events usually last for 4 to 12 h. The oscillations are usually strongest near the seafloor. An example of an ITB observed at MISO is shown in Fig. 2.

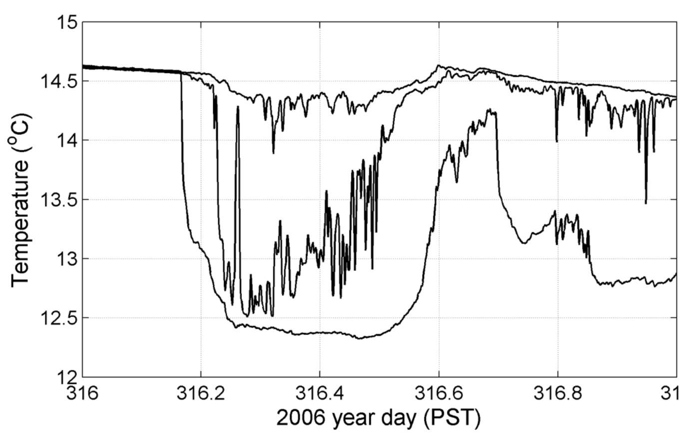

Fig. 2. Example of temperatures measured at MISO (12 Nov 2006). Temperatures measured by thermistors at 0.5 m, 5.4 m, and 8.5 m above the seafloor are shown by the lower, middle, and upper curves, respectively. Early in the day, the water column was homogeneous and relatively warm. Temperature decreased slowly until 316.2 PST (Pacific Standard Time) when it dropped very sharply. This drop was followed by highly energetic short period internal waves (solitons). At the end of the day, the water column again became more homogeneous and warmer.

The AUV surveys presented here were carried out just offshore of MISO (Fig. 1), so we reasoned that internal wave traveling across the survey area were likely to appear later at MISO. Our goal was to compare AUV data collected offshore with inshore record at MISO. This allowed us to investigate the propagation of internal waves over the shelf, in addition to our primary goal of verifying the efficacy of our survey method.

Assessment

The first AUV survey, 14-15 May 2007

The offshore and onshore points bounding the cross-shelf transect, as shown in Fig. 1, were 36.702°N, 121.935°W (water depth 97 m) and 36.685°N, 121.890°W (water depth 81 m), respectively. The transect was just inshore of a relatively steep part of the shelf break where nonlinear internal wave features were thought likely to appear. The seafloor slopes gently along the AUV transect, with no sharp topographic features.

On 14 May, the AUV was deployed from R/V *Zephyr* around 09:00 PDT (Pacific Daylight saving Time) at the inshore point. First, we ran a short AUV mission on a regular depth-bounded saw-tooth trajectory to measure the stratification of the water column. The data were then downloaded and quickly analyzed to define the temperature bounds of the thermocline (identified by where the temperature gradient was the highest). The lower and upper temperature bounds were set to 10.1°C and 10.3°C, respectively. Due to inertia, the vehicle overshot slightly beyond the temperature bounds, so the actual temperature envelope turned out to be thicker than programmed. At 15:00 PDT, the AUV was deployed for the overnight survey. On the next day, the AUV was recovered around 08:00 PDT after 18 full and two half transects.

Figure 3 displays the AUV's trajectory (in the vertical dimension) bounded by the 10.1°C and 10.3°C isotherms. During transects 1 to 4, isotherms descended 20 m at the inshore end of the transect. The most rapid change occurred between transects 1 and 2, when isotherms 1400 m from the inshore point dropped 22 m in approximately 1 h. This sharp drop may have been the leading edge of an ITB. Between transects 6 and 12, the isotherms rose back about 20 m, starting from the offshore end. The ITB seemed to be propagating shoreward across the shelf because the isotherms rose offshore first, and then inshore. In the last few transects, the isotherms dropped slightly and their depth stabilized.

Figure 4 shows that the depth of the 10.3°C isotherm varied substantially during the survey. The long-period (semidiurnal) oscillation is clearly shown in the middle panel of Fig. 5. The wavelength of this feature, which was possibly a propagating ITB, appears to have been much longer than the transect length (4.5 km), so it cannot be determined from these transects. The thickness of the layer between the two isotherms also changed rapidly during the survey. For example, the layer thickness at 2750 m distance in transect 4 was 20 m. Six hours later, in transect 10, the thickness decreased to 4 m. By 5 h later, during transect 16, the thickness was less than 1 m. These changes were probably the result of mixing caused by the ITB, by advection of water masses with different density structures or by compression or expansion associated with high vertical mode structure of nonlinear internal waves.

During transects 1 to 7, the density structure varied so much in the cross-shore dimension and changed so abruptly approximately halfway through the transect length, that we conclude that the AUV repeatedly crossed over a front between two different water masses. For example, on transect 4, offshore of the front, the average vertical temperature gradient was 0.01°C/m, but inshore of the front, the gradient was much higher (0.08°C/m). In comparison, the average vertical temperature gradient over the entire survey was 0.05°C/m. Isotherm depths varied substantially across the front. The 10.1°C isotherm inshore of the front was, on average, 10-m (and up to 25-m) deeper than that offshore of the front.

Many small internal wave oscillations were observed during the survey: in transects 2 to 6, between 0 and 2000 m; in transects 12 to 13, near 700 m; in transects 16 to 18, near 3500 m. In transect 2, a packet of small solitons (amplitude 5 m, wavelength 100 m) was observed near 700 m. In transects 4 and 5, a soliton (amplitude 6 m, wavelength 200 m) was also observed near 700 m.

The second AUV survey, 26-27 Nov 2007

The offshore and inshore points bounding the cross-shelf transect (Fig. 1) were 36.667°N, 121.922°W (water depth 85 m), and 36.638°N, 121.889°W (water depth 64 m) for the second survey. We first ran a short AUV mission on a regular depth-bounded saw-tooth trajectory to measure the stratification of the water column, and then quickly analyzed the data for defining the temperature bounds of the thermocline. As expected for late fall, the temperature gradient (0.02°C/m) was much weaker than during the May survey. Instead of a well-defined thermocline, there were two weak thermoclines. We set the lower and upper temperature bounds to 11.2°C and 11.6°C, respectively. At 15:20 PST, the AUV was deployed for the overnight survey. Around 06:00 PST on the next day, it was recovered after 16 full transects. The 0.4°C temperature envelope turned out to be too wide relative to the low thermal gradient. Consequently, the AUV's saw-tooth trajectory was not well constrained and did not follow the isotherm as closely as in the May survey. Hence the crossing rate (number of crossings of the thermocline in one transect) was much lower than that in the May surveys.

Despite our inability to define a clear thermocline and track internal wave features during November, the AUV survey was able to document large isotherm displacements throughout the survey (Fig. 6). The 11.2°C isotherm rose up to 22 m over the first 9 h of the survey, mostly in the inshore half of the transect. It then dropped nearly 15 m in the inshore half of the survey while rising rapidly in the offshore half. Between 11 and 14 h into the survey, the 11.2°C isotherm rose over 20 m at 3000 m. The thickness of the layer between the two

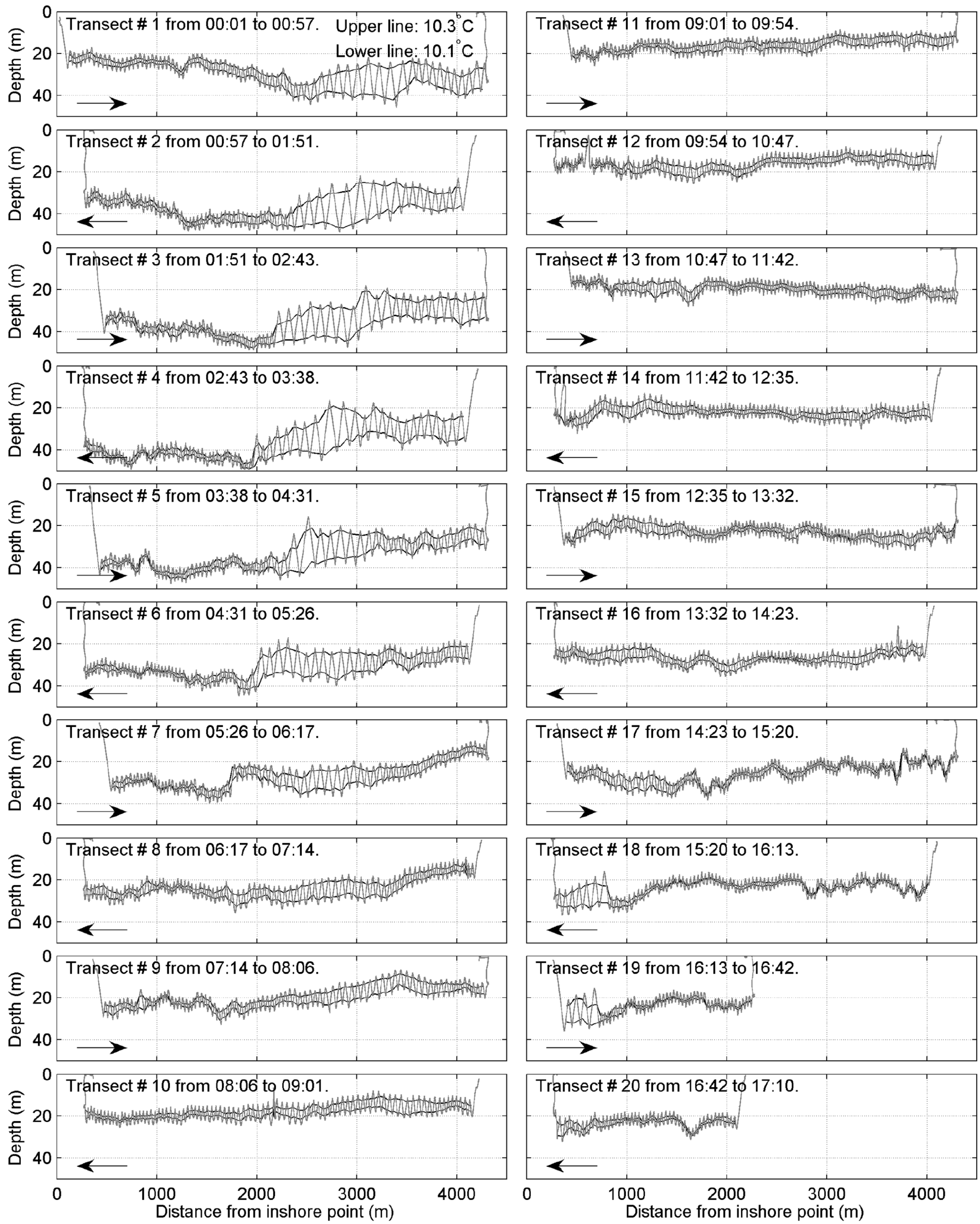

Fig. 3. The AUV transects in the 14-15 May 2007 survey. Gray saw-tooth line: the AUV's trajectory. Upper and lower black lines: the temperature bounds (10.1°C and 10.3°C). The arrow at the bottom of each plot shows the vehicle's traveling direction. The time on each plot is counted from the start of the survey.

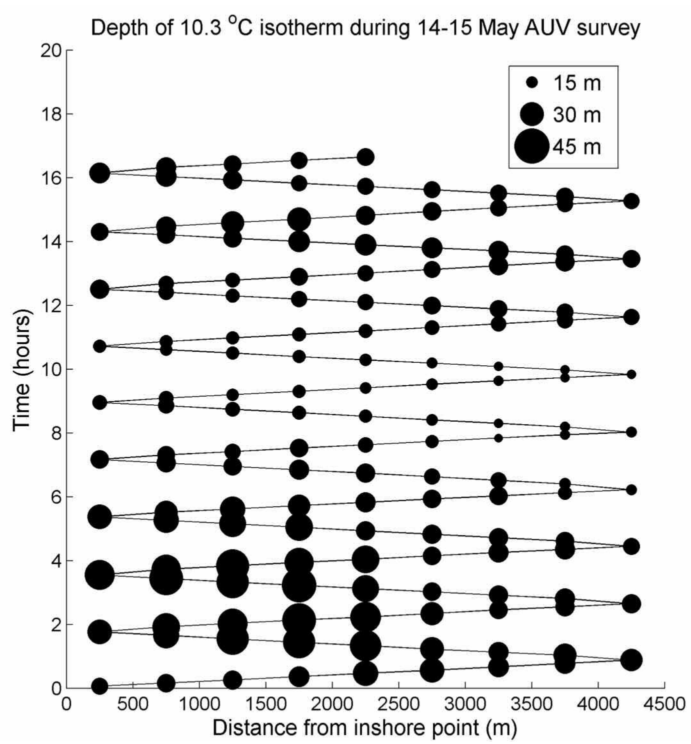

Fig. 4. The depth of the 10.3°C isotherm during the 14-15 May 2007 AUV survey. The line tracks the vehicle's distance from the inshore point. The diameter of each bubble is proportional to the depth of the 10.3°C isotherm, averaged over every 500 m along the transect. This figure highlights the substantial variation of the thermocline's depth with respect to time and location.

isotherms also changed rapidly throughout the survey. For example, the layer thickness at 500 m in transect 4 was 32 m. Eight hours later, it had thinned to 6 m. These changes may have been caused by the advection of water masses with disparate density structures

Comparison of AUV data and MISO data

Data from the 14-15 May 2007, AUV transects were compared with MISO mooring time series from the same time period. Figure 5 shows the tide level, the temperature at MISO, and the isotherm depth measured by the AUV, averaged over each transect. The relationships between the three data sets are quite clear. AUV-measured 10.4°C isotherm depth oscillated at the same frequency as the MISO temperature oscillation, and led the MISO temperature oscillation by approximately 2 h. At MISO, the tide level led the temperature oscillation by approximately 4 h. Note that rising isotherms over the mid-shelf generally coincide with rising isotherms at the inner shelf, consistent with the AUV and MISO both measuring a long-wavelength, low-mode semidiurnal tidal feature encompassing the majority of the narrow shelf. There are some indications of more nonlinear behavior at the inner shelf than at the outer and mid-shelf, including abrupt temperature changes and steep leading edges seen at MISO but not in the AUV time series.

Data from the 26-27 Nov 2007 AUV survey were also compared with MISO data, but their relationship is unclear, probably because of the relatively weak stratification, so we discuss this analysis no further.

Discussion

Oceanographers seek more effective ways to make measurements in the ocean. Sampling internal waves is particularly challenging because of the generally unpredictable and complex nature of these features. Traditional techniques either yield high-resolution time series at a single location (moorings or bottom mounted sensors) or limited measurements from multiple locations (shipboard measurements, images from airplanes and satellites). Observations from space or airplanes only give the wave's surface expression. Sampling from a ship gives low spatial resolution, and it is difficult to link events observed at different stations. AUVs, due to their mobility and cost-effectiveness, are a promising platform for making high-resolution measurement of internal waves over a large area.

Our goal was to develop and test a new technique for sampling internal waves, using an AUV. The vehicle was commanded to repeat a transect between two waypoints. Instead of the usual saw-tooth pattern between depth bounds, we programmed the AUV to fly within a narrow temperature envelope, thereby following a desired isotherm. Each AUV survey lasted up to 18 h. This is important because the long-wavelength oscillations, possibly ITBs, had periods near 12 h. During the May 2007 AUV survey, we were able to capture an entire ITB (Fig. 5) and documented a shoreward component of propagation. A longer survey would be even better, ideally covering several tidal cycles. This would be especially helpful for comparison with the long time series recorded at MISO. An additional benefit was the ability to determine that the wavelength (technically we measure the cross-shore component of wavenumber vector) of the high-frequency soliton-like features was approximately 100 to 200 m. This is important information that is difficult to estimate from spatially fixed mooring data.

The length of each AUV transect was approximately 4.5 km. This length was chosen for several reasons. First, 4.5 km was long enough for capturing an entire packet of solitons plus a significant distance before and after it, allowing for some ability to determine propagation along the transect. Second, 4.5 km was a reasonable distance for the AUV to navigate without coming to the surface for a GPS fix. Finally, it was the distance the AUV covers in approximately 1 h, a convenient figure. It proved to be an appropriate length. Even though it was not long enough to cover the entire wavelength of an ITB, it was long enough for observing the ITB's progression along the transect. As the AUV took about an hour to sweep the transect once, the temporal resolution was 2 h or less (the sampling interval at the transect's two ends were up to 2 h [Fig. 3]). In some cases, isopycnals were displaced so rapidly that the difference between one transect and the next was difficult to interpret. A longer transect, going

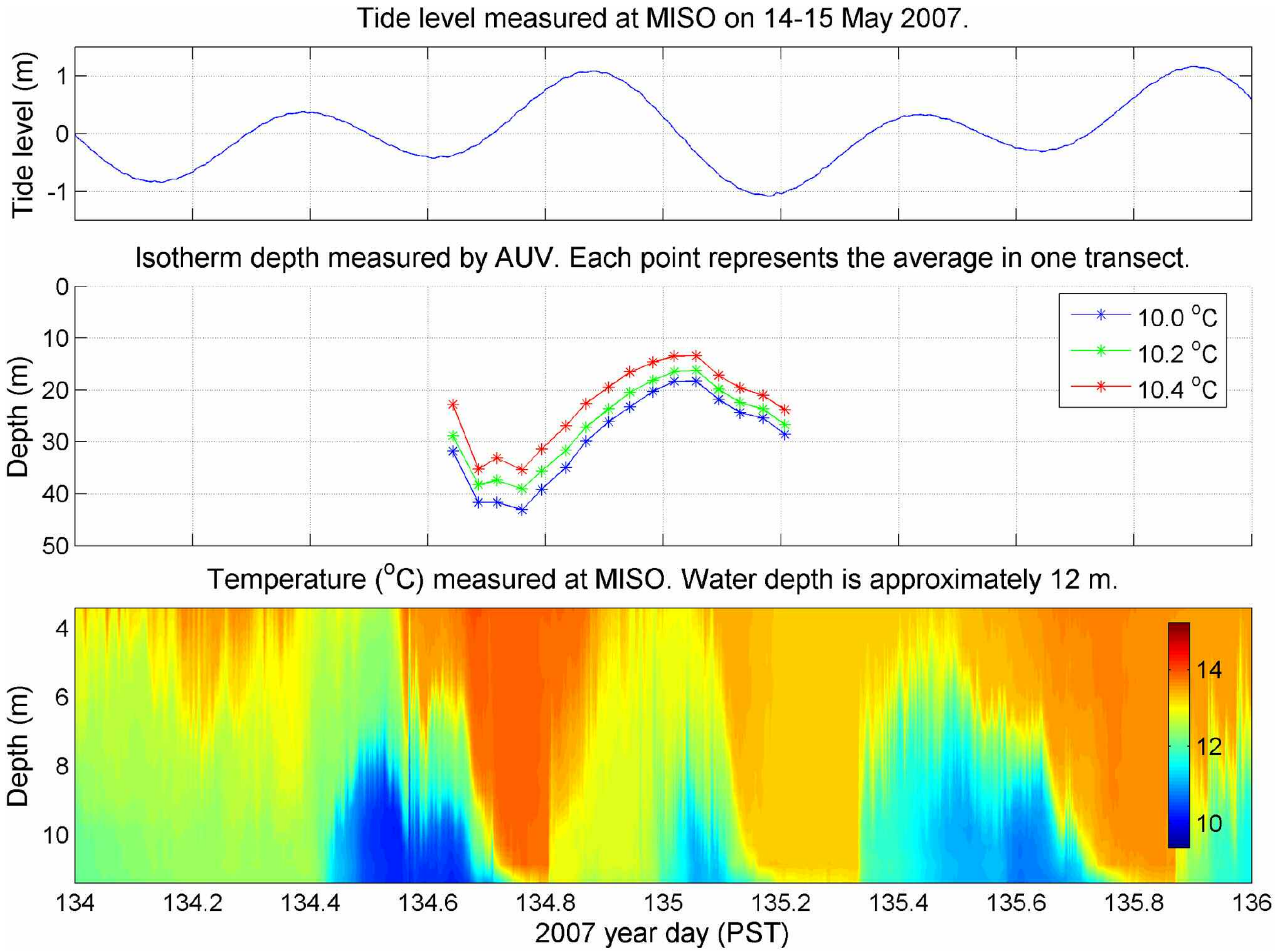

Fig. 5. Tide level and temperature measured at MISO and temperature measured by the AUV on the mid-shelf during the 14-15 May 2007 survey.

as far as the shelf break, or even farther offshore, could yield some interesting information about the evolution of ITBs over the shelf, but the temporal resolution would be lower. This problem might be solved by using multiple vehicles, each covering one section of a long transect.

For the AUV to sample internal waves efficiently, it must stay near the thermocline. The AUV's ability to do so depends on two factors: a proper flight-path angle and fast response to temperature changes. The AUV's flight-path angle (the angle between the vehicle's flight path and the horizontal) must be greater than the steepest possible slope of the thermocline so that it can always track it. According to a model based on KdV equations (Holloway et al. 1999), for conditions typical of Monterey Bay, CA when stratification is high (in summer and early fall), the slope of the thermocline can reach 13° (Fig. 7). Therefore the AUV's flight-path angle should not be lower than 13°. The AUV's flight-path angle was about 21° (in both descent and ascent) in the May 2007 survey, and it appeared to have worked very well. Figure 8 shows the AUV's trajectory and the isotherms of the temperature bounds. Between 1000-m and 1500-m (distance from the inshore point), the AUV sampled a steep soliton. The vehicle's flight-path angle was still much steeper than the slope of the soliton, so we conclude that the soliton was properly sampled. Another factor to take into account when selecting the flight-path angle is the AUV's steering capability. During the May 2007 survey, at a 21° flight-path angle, the AUV sometimes stalled out and lost steerage. We had to reduce the flight-path angle to 12° (in ascent) in the November 2007 survey to circumvent this problem (Fig. 9). Lowering the AUV's flight-path angle also slightly increased the vehicle's horizontal speed.

The AUV must react quickly to temperature changes to stay within the programmed temperature bounds. In this respect, the AUV performed very well. On average it overshot above or below the temperature bounds only by 2 m, mostly due to the vehicle's inertia and the limited steerage capability. It is important to adjust the width of the temperature bounds in accordance with the vertical temperature gradient. In the November 2007 survey, the width of the temperature bounds was too large for the low vertical temperature gradient, resulting in the AUV tracking the thermocline less closely than in the May 2007 survey.

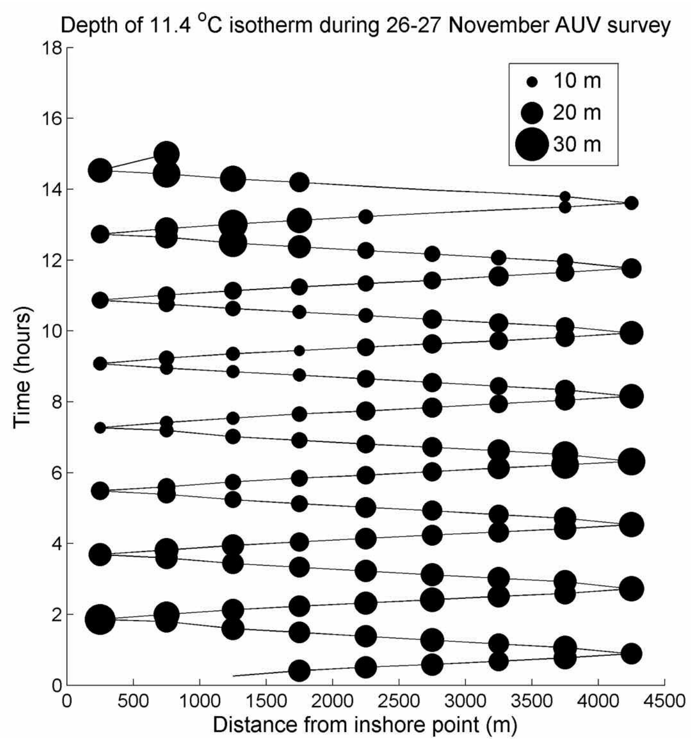

Fig. 6. The depth of the 11.4°C isotherm during the 26-27 Nov 2007 AUV survey. The line tracks the vehicle's distance from the inshore point. The diameter of each bubble is proportional to the depth of the 11.4°C isotherm, averaged over every 500 m along the transect.

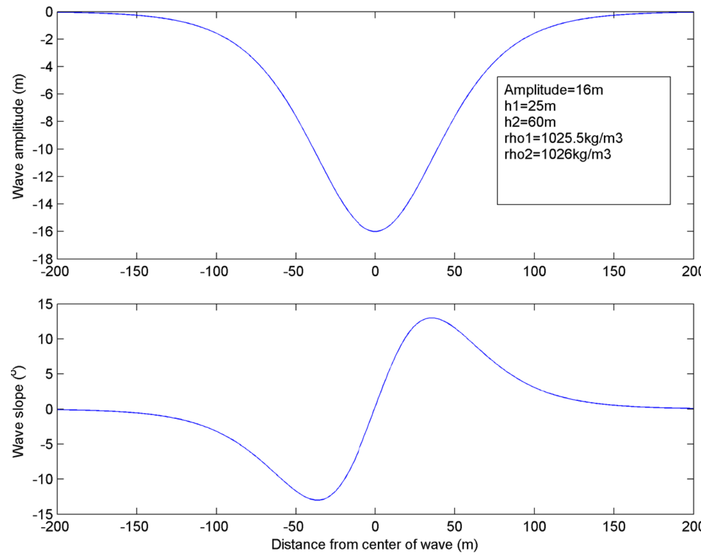

Fig. 7. The upper plot shows a KdV model of a nonlinear internal wave for conditions typical of Monterey Bay in late summer. The lower plot shows the slope of the same wave.

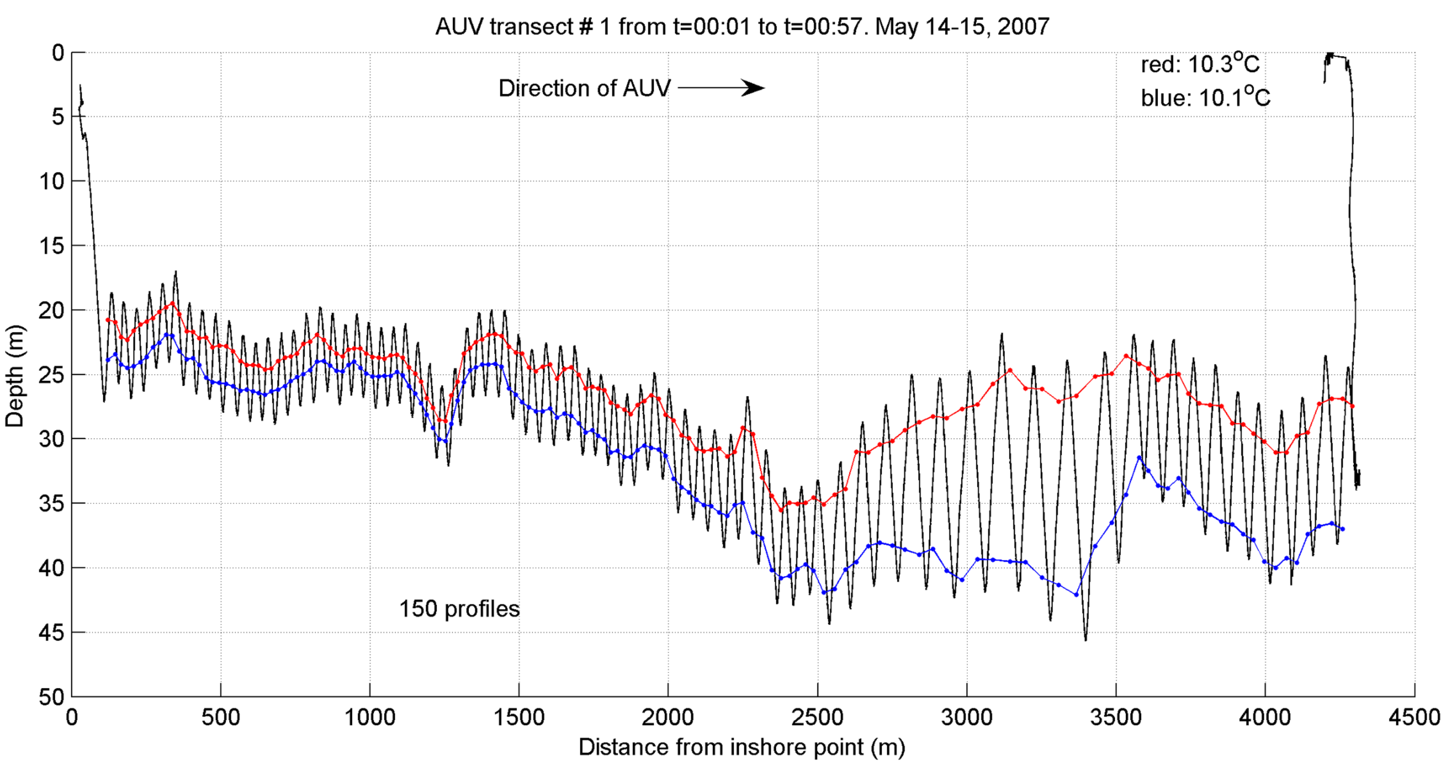

Fig. 8. The actual AUV trajectory (black line) and temperature bounds (red and blue lines) during the 14-15 May 2007 AUV survey.

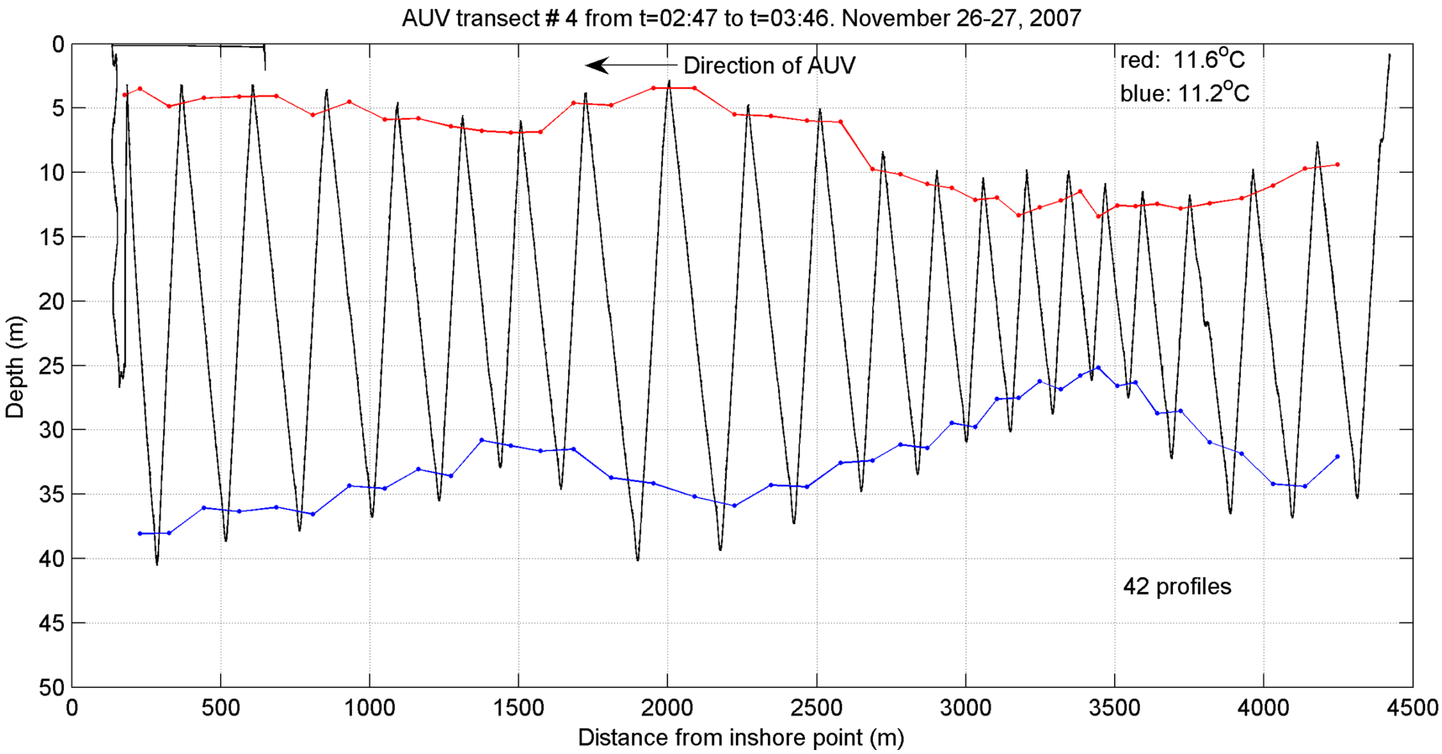

Fig. 9. The actual AUV trajectory (black line) and temperature bounds (red and blue lines) during the 26-27 Nov 2007 AUV survey.

The crossing rate (number of AUV crossings of the thermocline in one transect) depends directly on the vertical temperature gradient of the water column and the AUV's temperature bounds width. When the vertical temperature gradient is high and the temperature bounds width is small, the crossing rate is high. In the two AUV surveys discussed here, the horizontal spatial resolution (distance between two crossings of the thermocline) varied between 28.5 m and 100 m (Table 1). In the May 2007 survey, the crossing rate was much higher than that in the November 2007 survey. A high crossing rate is necessary for obtaining a precise image of the thermocline and capturing fine and steep features. A reduced width of the temperature bounds can increase the crossing rate, but the ultimate closeness of the two temperature bounds is limited by the AUV's control dynamics in the vertical plane.

Comments and recommendations

To enhance the AUV's sampling efficiency, one improvement would be to have the vehicle autonomously detect the thermocline and set the temperature bounds at the beginning of a long survey, instead of running a separate short mission prior to the survey. This would save time and allow for a launch from a distance (e.g., from an underwater docking station). In this scenario, the AUV first navigates to the survey region, makes depth-bounded profiles and determines the temperature bounds, and then starts the survey.

Ultimately, we want an AUV to be capable of detecting an internal wave, and then adapting its trajectory to track it, and making biological and chemical measurements around and within it. Tracking an internal wave requires knowing its direction of propagation. The main drawback of the repeated-transect approach presented in this article is that it only provides an approximate direction of the internal wave's propagation, but does not provide the actual angle of the direction (e.g., we cannot tell a northwestward propagation from a southwestward propagation). This problem could be solved by running an AUV on a V-shaped, triangular, or rectangular transect, or multiple vehicles on transects of different orientations. Designing the optimum configuration of transects is a study topic in itself. Tracking internal waves by AUVs could be very useful at places like the Luzon Strait in the South China Sea, where internal waves are highly predictable and steep (Ramp et al. 2004).

For reliable detection of internal waves, an AUV needs to be able to distinguish internal waves from other oceanographic processes. In Monterey Bay, for example, features such as fronts might easily be mistaken for internal waves. An AUV-based spectral classification method (Zhang et al. 2001) can be applied. When an AUV carries out a survey in an ocean field, it records a time series which mingles temporal and spatial variations of the field. The corresponding spectrum mingles the spectral information of time and space, as concisely expressed by the mingled-spectrum principle. The AUV speed determines the proportion of contributions from time and

Table 1. Characteristics of the AUV profiles. The width of the temperature bounds is defined as the difference between the upper and lower temperature bounds used for the AUV's thermocline tracking behavior. The average thickness (between the two temperature bounds), vertical temperature gradient, and crossing rate are the average values over the entire survey.

	Width of isotherm bounds (°C)	Average thickness (m)	Average vertical temperature gradient (°C/m)	Crossing rate (crossings/km)	Horizontal spatial resolution (m)
Survey 1	10.3-10.1 = 0.2	7.87	0.05	35	28.5
Survey 2	11.6-11.2 = 0.4	15.68	0.02	10	100

space. Consequently, the vehicle speed tunes the separability between the mingled spectra (as "seen" by the AUV) of different oceanographic processes. Based on this principle, we can select the optimum vehicle speed to achieve reliable classification of internal waves against other possible processes.

Conclusions

Long-wavelength, likely semidiurnal ITBs and high-frequency solitons, were the dominant features observed in the AUV surveys. ITBs observed at the mid-shelf had amplitudes ranging from 20 to 35 m and periods ranging from 5 to over 18 h. In the 14-15 May 2007 survey, we observed an ITB clearly propagating eastward (shoreward), presumably after originating at the shelf break or farther offshore. The amplitude of the solitons ranged from 4 to 16 m, and their periods were usually near 30 min. Some solitons appeared to be generated on the shelf, possibly as part of the dissipation of the ITBs. During the AUV surveys, the density structure changed dramatically in both space and time. The thermal gradient at the thermocline sometimes increased or decreased more than 10-fold within a tidal cycle. Fronts separating water masses with very different density structures were present intermittently during the surveys.

Overall, the AUV survey method presented in this paper was very effective. It yielded high-resolution information about isotherm displacements, and changes of the density structure near the thermocline: the horizontal spatial resolution was between 28.5 m and 100 m, and the temporal resolution was 2 h or less. We were able to identify internal tidal waves and calculate their amplitudes. AUVs have the potential to reveal much more information about internal waves, by using acoustic Doppler current profiler, chemical, and biological measurements, and by using improved sampling methods, as recommended here. Longer AUV surveys, possibly using a long-range AUV (Bellingham et al. 2010), would yield very useful data for understanding the evolution of ITBs on the shelf.

References

Bellingham, J. G., and others. 2000. An Arctic Basin observational capability using AUVs. Oceanography 13:64-71.

———, and others. 2010. Efficient propulsion for the tethys long-range autonomous underwater vehicle. *In* Proc. IEEE AUV'2010, Monterey, CA, U.S.A., September 2010. Institute of Electrical and Electronics Engineers. p. 1-6.

Bird, J. S., J. Ferguson, B. Laval, and P. Helland. 1997. AUV development for coastal marine science. *In* Proceedings of the 10th international symposium on unmanned untethered submersible technology. Durham, NH. Autonomous Undersea Systems Institute. p. 23-30.

Carter, G. S., M. C. Gregg, and R. C. Lien. 2005. Internal waves, solitary waves, and mixing on the Monterey Bay shelf. Cont. Shelf Res. 25:1499-1520.

Cheriton, O. M., M. A. McManus, M. T. Stacey, and J. V. Steinbuck 2009. Physical and biological controls on the maintenance and dissipation of a thin phytoplankton layer. Mar. Ecol. Progr. Ser. 378:55-69.

Colosi, J. A., R. C. Beardsley, J. F. Lynch, G. Gawarkiewicz, C. -S. Chiu, and A. Scotti. 2001. Observations of nonlinear internal waves on the outer New England continental shelf during the summer Shelfbreak Primer study. J. Geophys. Res. 106(C5):9587-9601.

Holloway, P. E., E. Peinovsky, and T. Talipova. 1999. A generalized Korteweg-de Vries model of internal tide transformation in the coastal zone. J. Geophys. Res. 104(C8):18333-18350.

Leichter, J., H. Stewart, and S. Miller. 2003. Episodic nutrient transport to Florida Coral Reefs. Limnol. Oceanogr. 48:1394-1407.

Lennert-Cody, C., and P. S. Franks. 2002. Fluorescence patches in high-frequency internal waves. Mar. Ecol. Progr. Ser. 235:29-42.

MacKinnon, J. A., and M. C. Gregg. 2003. Shear and baroclinic energy flux on the summer New England shelf. J. Phys. Oceanogr. 33:1462-1475.

McPhee-Shaw, E., D. Siegel, L. Washburn, M. Brzezinski, J. Jones, A. Leydecker, and M. Melack. 2007. Mechanisms for nutrient delivery to the inner shelf: Observations from the Santa Barbara Channel. Limnol. Oceanogr. 52:1748-1766.

Petruncio, E. T., L. K. Rosenfeld, and J. D. Paduan 1998. Observations of the internal tide in Monterey Canyon. J. Phys. Oceanogr. 28:1873-1903.

Ramp, S. R., and others. 2004. Internal solitons in the northeastern South China Sea. Part I: sources and deep water propagation. IEEE J. Ocean. Eng. 29:1157-1181.

Scotti, A., R. C. Beardsley, B. Butman, and J. Pineda. 2008. Shoaling of nonlinear internal waves in Massachusetts Bay. J. Geophys. Res. 113:C08031 [doi:10.1029/2008JC004726].

Small, J., and J. Martin. 2002. The generation of non-linear internal waves in the Gulf of Oman. Cont. Shelf Res. 22:1117-1128

Shroyer, E. L., J. N. Moum, and J. D. Nash. 2009: Observations of polarity reversal in shoaling nonlinear internal waves. J. Phys. Oceanogr. 39:691-701.

Stanton, T. P., and L. A. Ostrovsky. 1998. Observations of highly nonlinear internal solitons over the Continental Shelf. Geophys. Res. Lett. 25:2695-2698.

Thompson, D. R. 2007. AUV operations at MBARI, p. 1-6. Proc. MTS/IEEE Oceans'07. Marine Technology Society/Institute of Electrical and Electronics Engineers.

Tjoa, K. M. 2003. The bottom boundary layer under shoaling inner shelf solitons. M.S. thesis, Naval Postgraduate School.

Zhang, Y., A. B. Baggeroer, and J. G. Bellingham. 2001. Spectral-feature classification of oceanographic processes using an autonomous underwater vehicle. IEEE J. Oceanic Eng. 26:726-741.

Submitted 15 June 2011
Revised 27 October 2011
Accepted 17 November 2011